THE USE OF ULTRASOUND-TARGETED MICROBUBBLE DESTRUCTION IN

MEDIATED DELIVERY OF A GADOLINIUM-BASED MAGNETIC

RESONANCE IMAGING CONTRAST AGENT INTO

FIBROBLAST CELLS IN VITRO

APPROVED BY SUPERVISORY COMMITTEE

A. Dean Sherry, Ph.D. _____

Craig R. Malloy, M.D. _____

Peter Antich, Ph.D. _____

Robert Eberhart, Ph.D. _____

ACKNOWLEDGMENTS

THE USE OF ULTRASOUND-TARGETED MICROBUBBLE DESTRUCTION IN

MEDIATED DELIVERY OF A GADOLINIUM BASED MAGNETIC

RESONANCE IMAGING CONTRAST AGENT INTO

FIBROBLAST CELLS IN VITRO


by


C. HUNTER RUSSELL III


THESIS


Presented to the Faculty of the Graduate School of Biomedical Sciences

The University of Texas Southwestern Medical Center at Dallas

In Partial Fulfillment of the Requirements

For the Degree of


MASTER OF SCIENCE

The University of Texas Southwestern Medical Center at Dallas

Dallas, Texas

May, 2004

THE USE OF ULTRASOUND-TARGETED MICROBUBBLE DESTRUCTION IN

MEDIATED DELIVERY OF A GADOLINIUM BASED MAGNETIC

RESONANCE IMAGING CONTRAST AGENT INTO

FIBROBLAST CELLS IN VITRO

Publication No. _____

C. Hunter Russell III

The University of Texas Southwestern Medical Center at Dallas, 2004

Supervising Professor: A. Dean Sherry, Ph.D.

A method for delivering Gd-based MRI contrast agents by ultrasound-targeted microbubble destruction into fibroblast cells *in vitro* is presented. First, MRI contrast agents Gd-F-DOTP-ME and Gd-DOTA-4iBA are shown to associate with liposome microbubbles used as ultrasound contrast agents. Repeated washings with phosphate buffered saline followed by $T_1$ measurements at 20 MHz revealed Gd-DOTA-4iBA was retained more effectively by the liposome microbubbles. Secondly, ultrasound-targeted microbubble destruction using Optison™ microbubbles to deliver Gd-DOTA-4iBA into fibroblast cells displays negligible T1 shortening at 4.7T over controls. Further experiments are planned to validate these observations with other MRI contrast agents and other forms of microbubbles used for ultrasound image enhancement. The goal of these experiments is eventually combining MRI contrast agent delivery with ultrasound targeted microbubble destruction gene therapy to quantitatively determine the amount of DNA delivered into target tissues.

TABLE OF CONTENTS

# PRIOR PUBLICATIONS

Not Applicable

# LIST OF FIGURES

# LIST OF TABLES

# LIST OF DEFINITIONS

GdL – Gadolinium Ligands

Insonation – Ultrasonic irradiation

Insonification — Irradiation with sound

MRI – Magnetic Resonance Imaging

UCA – Ultrasound Contrast Agents

UTMD – Ultrasound Targeted Microbubble Destruction

# CHAPTER ONE
## Introduction

1. <u>**Background**</u>

Current advancements in gene therapy and delivery modalities are limited by the lack of an accurate way to quantify the amount of DNA in a gene payload delivered to target tissues from delivery agents. Quantification techniques of gene therapy currently employed in animal and tissue culture models rely on detecting the post transfection gene expression protein products or mRNA transcripts. While active gene expression is the ultimate goal of therapy, the time consuming post transfection wait period for uptake and expression does not provide immediate feedback on the efficiency of the delivery mechanism itself. Additionally, the detection of successful transfection in animal models frequently requires sacrificing the experimental animals. If a new gene delivery modality is under investigation, evaluation of the new approach may be hindered if the batch of DNA being delivered is low in activity or inactive. Therefore, a need exists to directly link DNA delivery during gene transfection to a reporter agent which can be directly and immediately detected, post transfection delivery into tissue cells. The ultimate goal of the series of experiments being presented is to eventually combine gadolinium (Gd) based magnetic resonance imaging (MRI) contrast agent delivery with ultrasound targeted microbubble destruction (UTMD) gene therapy to quantitatively determine the amount of DNA delivered into the target tissues. If the MRI contrast agents can be successfully incorporated into or associated with delivery vesicles carrying the gene

payload, then post transfection MR imaging may allow for direct correlation of DNA delivered to cells with Gd contrast agent image enhancement. Additional insight could be gained from these experiments regarding the biological effects of gadolinium based MRI contrast agents as current information on how Gd compounds interact within tissues in vivo is incomplete.

### 1.1. UTMD: The Need for Improved Drug and Gene Delivery Mechanisms

Often during the course of therapeutic intervention, there arises difficulty in injection of therapeutic agents into hard-to-reach human tissues or there is a risk of organ damage from movement of the target organ. Additionally, bolus injection with a syringe may not effectively distribute the drug within the tissues of the target organ. For example, DNA transfection requires penetration of most of the cell membranes within the targeted tissues of an organ in order to replace the defective genes. These issues have led to the search for a new method of delivery of therapeutic drugs and genes directly into a target tissue region (and in the case of genes, directly through the cell membranes of the tissue).

UTMD has shown promise as a possible gene therapy and drug delivery tool. Recent research [1, 2] has shown that encapsulated microbubbles used as ultrasound contrast agents have the capacity to be used as delivery vesicles by loading them with therapeutic genes (or drugs). Effective delivery strategies involve localized release of a gene payload to a specific tissue of interest by targeted ultrasonic destruction of these microbubble carriers.

UTMD delivery is advantageous over other gene/drug delivery methods for several reasons. Foremost, packaging the gene payload may protect it from inactivation and removal

as the microbubble encapsulating material shields its DNA content from destruction by circulating endonucleases. Secondly, the ability to target these delivery vesicles to regions of disease allows for the site-specific delivery of therapeutic genes, or drugs, to that damaged tissue only.  A further factor enhancing therapeutic agent delivery is the phenomenon of sonoporation. By carefully controlling the intensity with which the bubbles burst, small cavitation-induced perforations can be made in nearby cell membranes, permitting infiltration of the DNA or therapeutic agents directly into cells of the target tissue. The underlying principles causing sonoporation will be discussed in greater detail in the next section.

# CHAPTER TWO
# Review of the Literature

## OVERVIEW OF ULTRASOUND & MRI CONTRAST AGENTS

### 2. Microbubbles: Creation and Use as Ultrasound Contrast Agents

Microbubbles have been used for years as contrast agents in ultrasound imaging (Ultrasound Contrast Agents or UCA) to improve vascular resolution [3, 4] by inducing an acoustic impedance mismatch between fluids contained within the vascular lumen or heart chambers and the surrounding tissues. In comparison to the other contrast agents used in many imaging modalities, microbubbles are affected by the intensity of the applied field used for imaging. Microbubbles can be destroyed when subjected to an ultrasound field of sufficiently high peak pressure, leading to a release of reflected acoustical energy containing many harmonics which are often used to further enhance image contrast [3].

Within the bloodstream, microbubbles can be generated in situ when blood is exposed to sufficiently high ultrasound peak pressure. However, very high ultrasound pressures can induce hemolysis and cause tissue damage [5-7]. A dimensionless parameter called the Mechanical Index (MI) is used as a predictor of possible biological effects arising from cavitation mechanisms. MI is defined as [8]:

$$\text{Mechanical Index} \equiv \text{MI} \equiv \frac{P_r}{\sqrt{f}}$$

where $P_r$ is peak rarefaction (negative) pressure in MPa (megapascals), and $f$ is the frequency in MHz. Clinical imaging parameters thought to be generally safe for use [3] are a Mechanical Index (MI) of less than 2.

4

Microbubble formation in the bloodstream in situ is possible through ultrasound-induced cavitation, which is observed at sufficiently high Mechanical Index values. As microbubbles are exposed to the ultrasonic radiation, initiation of the cavitation process depends substantially on the existence of "nuclei" in a fluid medium, with most natural liquids (in this case blood) meeting this requirement. These nuclei are in essence small gas bodies which are dissolved in blood or associated with the surfaces of organic molecules [8]. The more "nuclei" present in the blood, the smaller the wave intensity needed for initiation of cavitation.

Cavitation mechanisms can be classified as stable or inertial (transient). Stable cavitation relates to bubbles that oscillate linearly around some equilibrium radius and can persist in the circulation for a longer period of time (several acoustic cycles) [9] . Inertial cavitation is the mechanism by which bubbles formed in a liquid oscillate wildly, experience rapid contraction to the point of collapse, then rebound violently, generating shockwaves that may lead to mechanical damage of surrounding tissues [10, 11] and hemolysis. Research into the biological effects of ultrasound has given  support to the idea that the disruptive effects of the cavitation mechanisms [12, 13] and /or the microstreaming [12] observed from microbubble translocation during insonation are responsible for the sonoporation phenomenon.

For imaging purposes, bubbles created through inertial cavitation tend to be too small, highly unstable, and of limited persistence in the blood-- lifetime on the order of several milliseconds [14] -- to be effectively used for image enhancement.

To overcome these problems, considerable effort has been put forth over the past decade to develop externally synthesized, encapsulated microbubbles for injection into the bloodstream as ultrasound imaging contrast agents. Intravenously injectable encapsulated microbubbles now commercially available, such as the albumin based UCA Optison™, are effective ultrasound contrast agents at ultrasound wave intensity levels much lower than those required to form bubbles in situ through fluid cavitation [3]. Current generations of externally produced microbubbles are synthesized to possess an ideal diameter (roughly 3μm) allowing unimpeded passage throughout the circulation (including capillaries and the lungs), resonate at commonly used ultrasound frequencies (roughly 3 MHz) for good echo contrast, and to persist in the bloodstream long enough for imaging to take place (on the order of minutes) [3].

## 2.1    The Role of Gadolinium (III) Chelates in Magnetic Resonance Imaging

Magnetic Resonance Imaging has proven to be one of the most efficient and least invasive tools for diagnosing diseases and for imaging various biological processes at the tissue or even cellular level. The imaging definition of the biological systems, tissues, and organs being examined is greatly enhanced by MRI contrast agents. These agents function by heightening the intrinsic differences in the $1/T_1$ (spin-lattice or longitudinal relaxation) and $1/T_2$ (spin-spin) relaxation rates which, in conjunction with water concentration, give rise to the signals used for image generation by a MRI Spectrometer. Gadolinium ($Gd^{3+}$) is the most frequently chosen metal atom to be bound to ligands (GdL) for use as contrast agents (CA) because it possesses a very high magnetic moment and high relaxation efficiency. The

solvent (diamagnetic) and the $Gd^{3+}$ complex (paramagnetic) contributions to the relaxation rates of solutions are given by equation [15]:

$$\left(\frac{1}{T_1}\right)_{obsd} = \left(\frac{1}{T_1}\right)_d + \left(\frac{1}{T_1}\right)_p \qquad (1)$$

where $(1/T_1)_{obsd}$ is the overall observed relaxation rate in the presence of the $Gd^{3+}$ complex, $(1/T_1)_d$ is the solvent (diamagnetic) relaxation rate in absence of GdL ($1/2.7=0.33$ $s^{-1}$) and $(1/T_1)_p$ is the paramagnetic contribution to relaxivity of the $Gd^{3+}$ complex.

In the absence of solute-solute interactions, this equation can be re-expressed in terms of relaxivity ($R_1$) and concentration of the $Gd^{3+}$ complex $[GdL]_{Total}$, where $R_1$ has units of $mM^{-1}s^{-1}$ and $[GdL]$ is in mM.

$$\left(\frac{1}{T_1}\right)_{obsd} = \left(\frac{1}{T_1}\right)_d + R_1[GdL]_{Total} \qquad (2)$$

There are two components that contribute to water relaxation enhancement by a paramagnetic GdL complex: inner-sphere, $R_{1i}$, which results from the direct lanthanide-water proton interactions, and outer-sphere, $R_{1o}$, which is the sum total of the contributions from bulk water protons unbound to the lanthanide ion. $R_{1o}$ contributions to relaxivity may be assumed constant for GdLs of similar size and ligand structure where as $R_{1i}$ can vary substantially according to the various structural parameters of $Gd^{3+}$ complexes. The $R_{1i}$ contribution is given by the following equations [15]:

$$R_{1i} = \frac{Bq\,\tau_c}{a^6} \qquad (3)$$

$$\tau_c^{-1} = \tau_s^{-1} + \tau_m^{-1} + \tau_r^{-1} \qquad (4)$$

In equation (3) $B$ is the fixed magnetic field strength, $\underline{a}$ is the metal-proton distance, $\underline{q}$ is the metal-coordinated water number, and $\tau_C$ is the overall correlation time. The parameter $\tau_C$, from equation (4), is the sum of the electronic relaxation time, $\tau_s$, the water exchange time, $\tau_m$, and the molecular rotational correlation time, $\tau_r$, of the $Gd^{3+}$ complex

# CHAPTER THREE
## Methodology

**3**     <u>Synthesis of GdL Loaded Liposome Microbubbles & T1 Measurements</u>
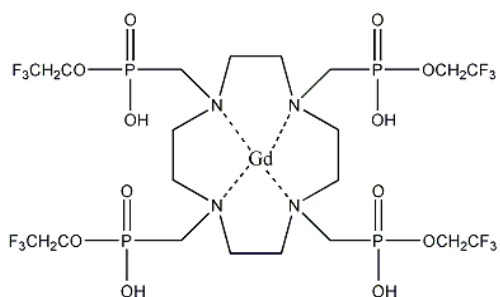


**Figure 1. Gd(F-DOTPME)**
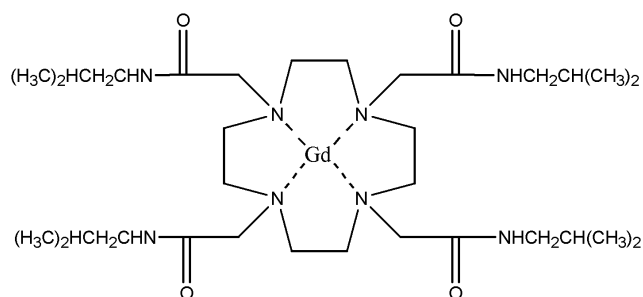


**Figure 2. GdDOTA-4iBA**
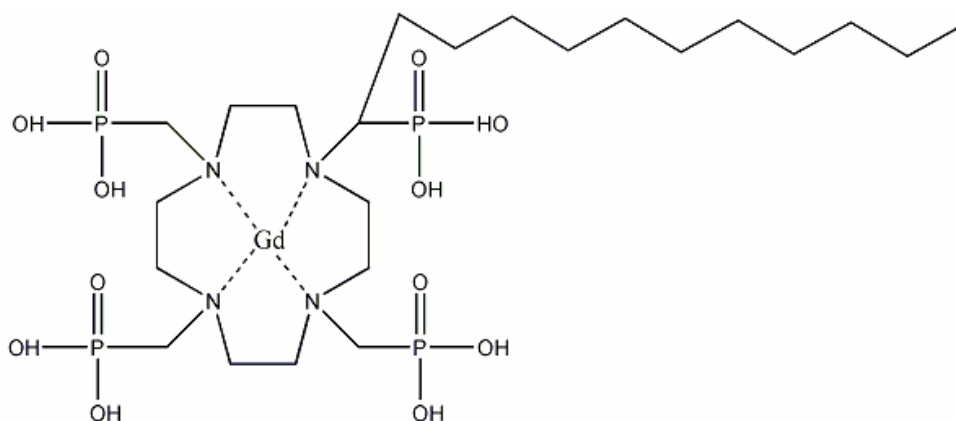


**Figure 3. Gd(C11-DOTP)**
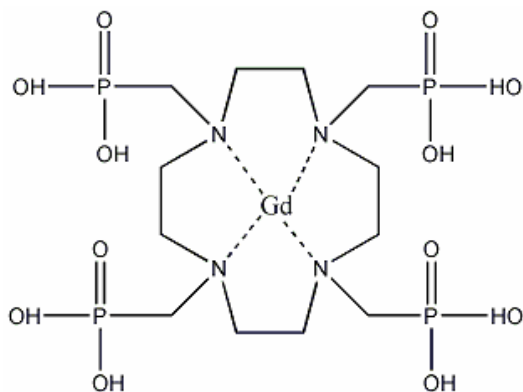
**Figure 4. Gd-DOTP**

The first phase of the research being presented was to investigate the stability of

incorporating Gd-F-DOTP-ME, GdDOTA-4iBA, Gd(C_{11}-DOTP), and Gd-DOTP into

microbubbles containing perfluoropropane encapsulated within: (1) a liposome shell and (2)

a shell of sterile human serum albumin

## 3.1   Preparation of Liposome UCA Containing GdL & Stability Analysis

A solution of 0.4% 1, 2-dipalmitoyl-sn-glycero-3-phosphatidylcholine (Sigma, St.

Louis, MO), 0.1% 1, 2-dipalmitoyl-sn-glycero-3-phosphatidyl ethanolamine, (Sigma, St.

Louis, MO), and 10% glycerol was diluted in phosphate buffered saline (PBS) at pH 7.4 and

mixed with either Gd-F-DOTP-ME, GdDOTA-4iBA, or Gd(C_{11}-DOTP)    (all three

compounds provided by the lab of A.D. Sherry, PhD, U.T. Dallas) to yield 5mM GdL in the liposome UCA solutions. Aliquots of 0.5 mL of this GdL-UCA solution were placed in 1.5 mL eppendorf vials; the remaining headspace was saturated with the perfluoropropane gas (Air Products, Inc, Allentown, PA). Each vial was then mechanically shaken for 20 seconds in a Vialmix™ (Bristol-Myers Squibb Medical Imaging, Inc., North Billerica, MA). After the solution is allowed to sit undisturbed for 5 minutes, the GdL-liposome microbubbles appear as a milky white suspension floating on the top of a liquid layer consisting of unformed liposome reagents and unbound GdL. A 200 μL aliquot of the subnatant was retained for $T_1$ measurements, the rest was discarded. The mean diameter and concentration of the Gd-DOTA-4iBA loaded microbubbles in the upper layer were measured by Multisizer 3 Coulter Counter® (Beckman Coulter, Inc., Fullerton, CA) and were $1.55 \pm 1.205$ μm and $9.39 \times 10^9$ GdL-liposome microbubbles/ mL, respectively. The physical characteristics of the Gd-F-DOTP-ME loaded microbubbles showed a mean diameter of $1.863 \pm 1.205$ μm and concentration of $9.22 \times 10^9$ microbubbles /mL, while $Gd(C_{11}-DOTP)$ loaded microbubbles possessed mean diameter of $1.412 \pm 0.934$ μm with a concentration of $12.7 \times 10^9$ microbubbles/mL. Synthesis of liposome microbubbles containing $Gd(C_{11}-DOTP)$ was unachievable at the 5 mM GdL concentration. While a small layer of bubbles was noted upon synthesis of $Gd(C_{11}-DOTP)$ loaded microbubbles at a 2.5 mM GdL concentration (mean diameter $=1.412 \pm 0.934$ μm, concentration $= 12.7 \times 10^9$ microbubbles/mL), these microbubbles were short lived and had almost completely disappeared under visual microscopic inspection  after 2 hours of refrigeration at 4°C. The other GdL loaded

microbubbles were stable and under microscopic inspection, displaying normal size microbubbles after 24 hours refrigeration.

### 3.2    Preparation of Albumin Microbubbles Containing GdL

A solution containing 5% dextrose (Sigma-Aldrich, St Louis, MO), 5% sterile human serum albumin (ICN, Costa Mesa, CA) was mixed with solutions of either, Gd-F-DOTP-ME, GdDOTA-4iBA, and Gd(C$_{11}$-DOTP)  for a total volume of 2 mL and final GdL concentrations of 4.6 mM Gd-F-DOTP-ME, 4.6 mM GdDOTA-4iBA, and 5.0 mM Gd(C$_{11}$-DOTP).  The GdL − albumin solution was drawn into a 20-mL Monoject syringe which would be used as a reaction vessel for the sonication process to form the microbubbles. The Leur-Lok of this syringe was then connected to a 3-way stopcock and the plunger of the syringe removed so the tip of 0.5 inch horn transducer of the Misonix Sonicator® 3000 (Misonix, Farmingdale, NY, USA) could be immersed just below the surface of the dextrose-albumin solution. Additionally, the temperature probe of the sonicator was inserted into the solution. A 4 mL aliquot of perfluoropropane was drawn into a 5 mL Monoject syringe and attached to the 3-way stopcock at the base of the reaction vessel. The user controlled dial of the sonicator interface was preset to level 9 for high intensity sonication with a converter/horn frequency of 20 kHz and a controlled cutoff temperature set at 72°C. As sonication was performed there was concurrent injection of perfluoropropane gas into the solution, continuously over a 20 second interval. During sonication, the solution became a white, frothy mixture of microbubbles beneath a layer of foam with some residual mixture

clinging to the sonicator probe. In order to collect as much of the mixture as possible, the probe was rinsed off with 2 mL of PBS which was collected into the reaction vessel. This mixture was transferred to a 15 mL polystyrene tube and refrigerated at 4°C for a minimum of 2 hours to allow for complete microbubble separation from the mixture.

### 3.3    Results of Albumin GdL -Microbubble Synthesis and Stability Analysis

Samples were taken from the microbubble layer of each solution after 2 hours and 24 hours for concentration and particle size determination using the Coulter Counter. After 2 hours, all three of the GdL- microbubble solutions had mean particle diameter with in the ideal range of 2-4 µm. The GdDOTA-4iBA microbubbles were slightly on the high end of this ideal range with a mean diameter of 4.665 µm. Microbubble stability varied amongst the compounds under investigation after 24 hours.

- **Gd-DOTA-4iBA  Loaded Microbubbles**

    Albumin microbubbles made with **GdDOTA-4iBA** had mean diameter increase from 4.665 µm to 6.443 µm with a simultaneous increase in the particle concentration from 334.7E6/ mL to 910.7E6/ mL. This indicates microbubble formation was still occurring during the overnight incubation and the microbubbles were swelling in size. Size enlargement is also observed from the increase in percentage of microbubbles greater than 4 µm, which increased from 49.6% after 2 hours to 67.2% after 24 hours.

- **Gd-F-DOTP-ME Loaded Microbubbles**

After 24 hours, the diameter of albumin microbubbles synthesized with the Gd-F-DOTPME dropped from 3.217 μm to 1.278 μm with a corresponding dramatic decrease of particles with diameter in excess of 2 μm from 58.4% to 5.2%. This indicates microbubbles synthesized with Gd-F-DOTPME are not stable when stored for 24 hours.

- **Gd ($C_{11}$-DOTP) Loaded Microbubbles**

Those albumin microbubbles synthesized with Gd($C_{11}$-DOTP) show the greatest stability during overnight refrigeration. There is only a slight increase in mean bubble diameter and percentage of bubbles in excess of 4 μm in diameter, but there is a notable increase in the number of microbubbles with diameters greater than 2 μm, from 52.9% after 2 hours to 100% after 24 hours refrigeration. This is also reflected in the significant decrease in particle concentration, which dropped by 82% after 24 hours, implying more microbubble formation is occurring and yielding microbubbles in the ideal diameter range. Prior investigations into the affinity of Gd($C_{11}$-DOTP) for albumin have been reported [16].

### 3.4    *Determination of Albumin binding constant for GdDOTA-4iBA*

GdDOTA-4iBA binding affinity for albumin was performed. Using bovine serum albumin (BSA) in essentially fatty acid free (0.001% FA), lyophilized powder form [Sigma Aldrich, St. Louis, MO], a 5mM BSA stock solution with 2.59mM GdDOTA-4iBA was made. A 200 μL working solution of 2.50mM GdDOTA-4iBA without albumin was used to

start the $T_1$ measurement process. $T_1$ measurements were obtained using a 20 MHz NMR analyzer and a standard inversion recovery pulse sequence at 25°C. After the initial $T_1$ value was recorded, 5 μL from the stock BSA-GdL solution was mixed into the working solution, after which the $T_1$ value was recorded. This process was repeated through multiple iterations until enough data points had been collected for curve fitting and binding constant determination. Binding constant determination depends upon the following binding relationships between GdL and albumin

$$K = \frac{[GdL \cdot BSA]}{[GdL] \cdot [BSA]}$$

$$[GdL]_{Total} = [GdL]_{free} + [GdL \cdot BSA]_{Bound}$$
$$[BSA]_{Total} = [BSA]_{free} + [GdL \cdot BSA]_{Bound}$$

The above equations fit into the following relationship, a modification of eq.2, between observed $T_1$ values and [GdL] [BSA] binding

$$\frac{1}{T_{1\_obs}} = \left( r_{1,free} * [GdL]_{free} + r_{1,bound} * [GdL \cdot BSA]_{bound} \right) + \frac{1}{T_{dia}} \qquad \text{(Eq. 2.4.1)}$$

The observed $T_1$ values were fitted to projected values of a 1:1 binding model generated using PSI-PLOT [version 7.5, Poly Software International, Inc., USA] with bound $r_1$ [BSA] [GdL] = 23.5 mM$^{-1}$s$^{-1}$, free $r_1$ [GdL] = 6.7 mM$^{-1}$s$^{-1}$, and K= 0.6 mM$^{-1}$ These parameters were based on the parameters for a compound similar to GdDOTA-4iBA with known binding properties. Results of the $T_1$ acquisition and fitting are shown in (Figure 5). A "goodness of fit" coefficient of 0.99 is observed between the projected values (1/$T_1$ calculated) and the observed values (1/$T_1$ experimental), indicating the used parameters offer a near perfect

model of binding affinity to albumin. It is technically not correct to refer to this as a true "binding constant" since there is no process to differentiate out the number of binding sites on albumin being occupied by GdDOTA-4iBA. Therefore, this model only holds if the assumption is one-to-one binding.
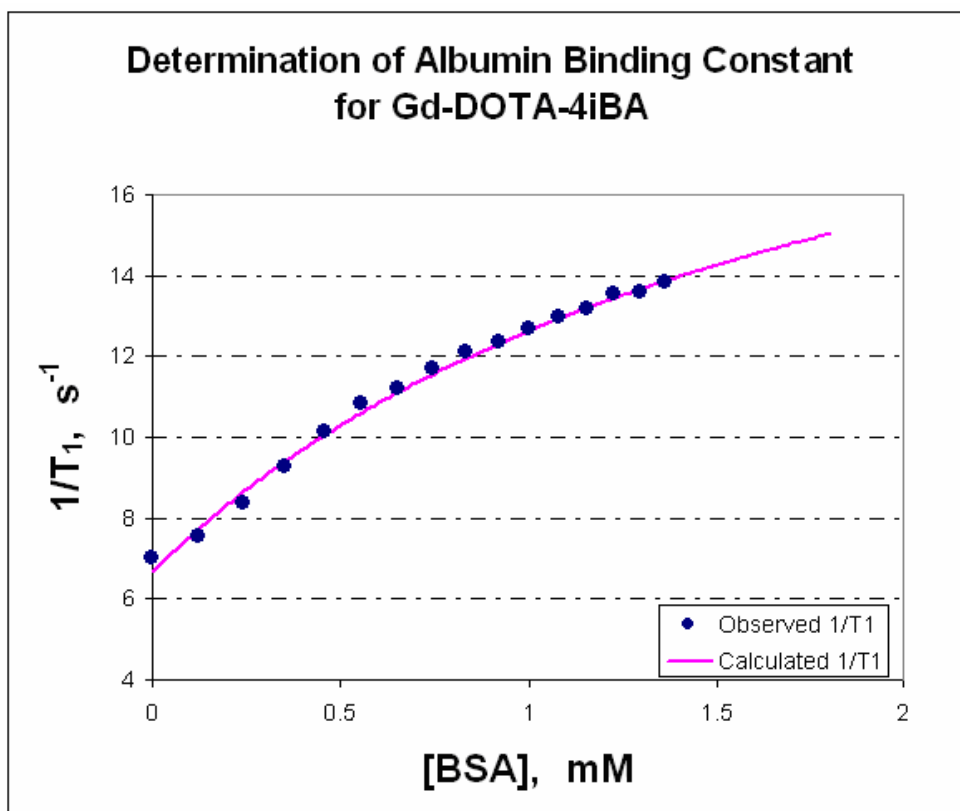


**Figure 5. Determination of Albumin Binding Constant for Gd-DOTA-4iBA**

### 3.5  Spin-lattice relaxation time (T1) measurements of GdL loaded UCA solutions

In addition to the 5 mM GdL-liposome samples prepared above, a 1mM Gd-F-DOTPME — liposome microbubble preparation and a 1 mM GdDOTP – liposome

microbubble preparation were made for comparison using the same protocol described above.

An aliquot of 100 µL was taken from each of the GdL-UCA suspensions and placed in 10x75 mm disposable borosilicate glass culture tubes for $T_1$ measurements.

$T_1$ measurements were obtained using a 20 MHz NMR analyzer and a standard inversion recovery pulse sequence at 25°C. In order to determine the extent to which the GdL compounds associate with and are retained by the liposome microbubbles, the GdL-UCA solutions were subjected to multiple washings with phosphate buffered saline (PBS). After each $T_1$ measurement was recorded, the GdL-UCA samples were washed with 200 µL of PBS, allowed to re-separate, followed by removal of the subnatant PBS wash from the glass tube. The washed samples were subsequently measured for $T_1$ values, as were the corresponding PBS washes and the original subnatant 200 µL aliquot from GdL-UCA synthesis. Multiple iterations of this wash and $T_1$ acquisition process were performed

### 3.6    GdL-Loaded Liposome UCA Synthesis Results & Discussion

The values displayed in (Figure 6) and (Figure 7) show the measured $T_1$ time with respect to the number of PBS washes. With each successive wash cycle, the measured $T_1$ values increased for both the GdL-UCA, the 1mM GdDOTP microbubbles and the PBS washes for all GdL compounds. Of the two Gd-conjugates under investigation, the Gd-DOTA-4i-BA loaded microbubbles (Figure 6) exhibit a much slower rate of $T_1$ increase post PBS washing, only increasing by a factor of 5 after the first wash (from 35.16 sec to 183.4 sec), whereas the $T_1$ reading for the Gd-F-DOTP-ME sample (Figure 7) has increased over

17 fold after the same number of washes (from 58.7 sec to 1033.5 sec). There also appears to be a point after the 2$^{nd}$ wash where the amount of Gd-F-DOTP-ME retained in the microbubble is equivalent for both the 1mM & 5mM suspension. This implies that the amount of extra Gd-F-DOTP-ME incorporated into the microbubble in the 5mM suspension, is loosely associated and is released quickly into the wash. Both compounds under investigation show favorable binding to liposome microbubbles when compared to the 1mM Gd-DOTP complexed microbubbles (Figure 8). Each successive PBS wash releases a nearly equivalent amount of Gd-DOTP into the wash, as is retained in the microbubble.
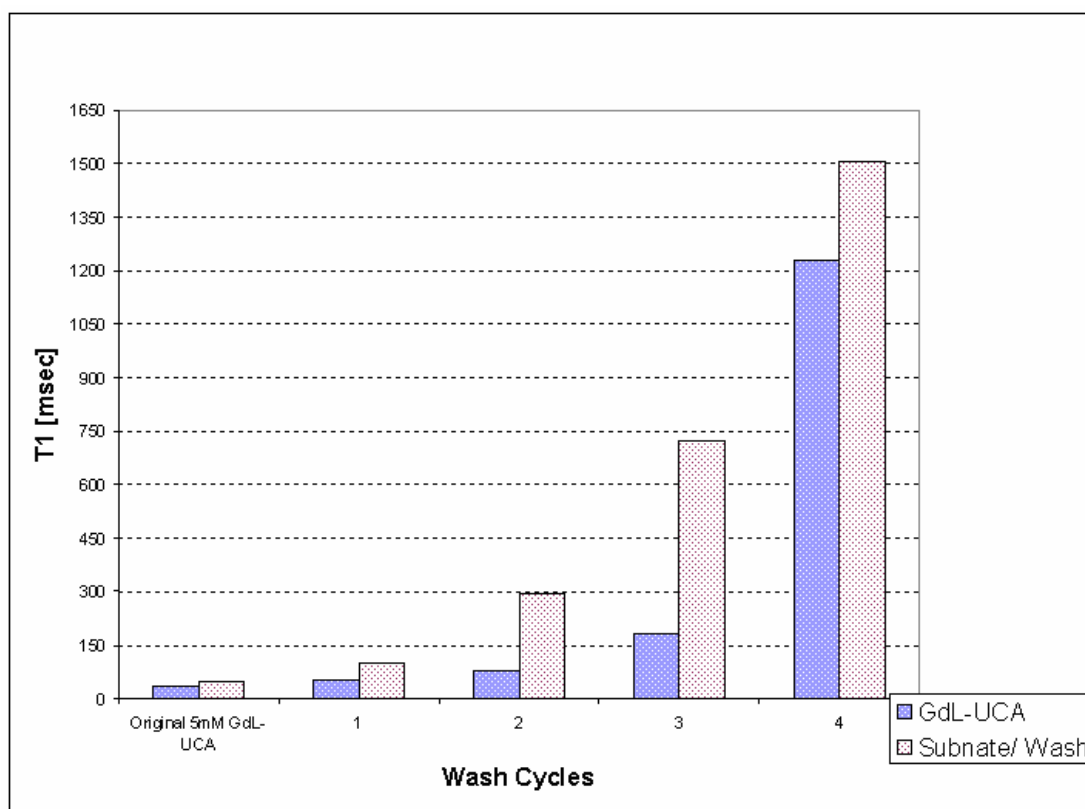


**Figure 6. Post Wash T$_1$ Measurements of 5mM Gd-DOTA-4i-BA Liposome Microbubble Suspension**
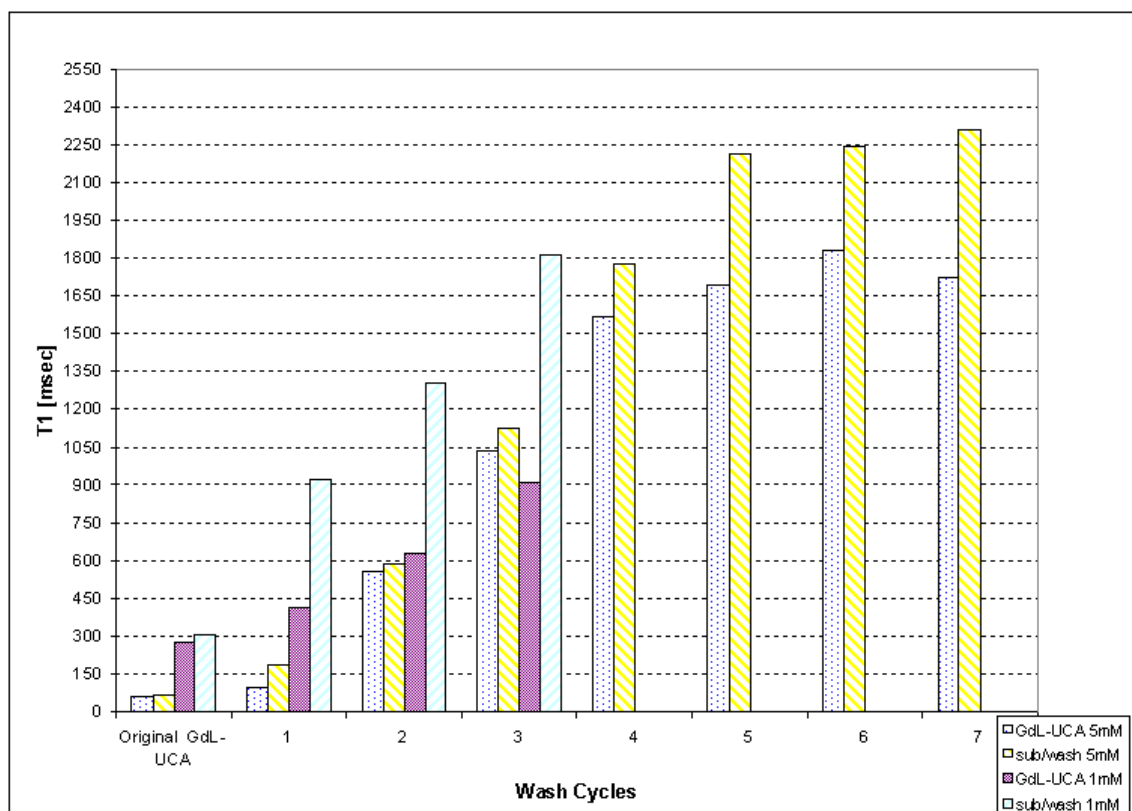
**Figure 7. Post Wash T$_1$ measurements of 1 mM & 5 mM Gd-F-DOTP-ME Liposome Microbubble Suspensions**
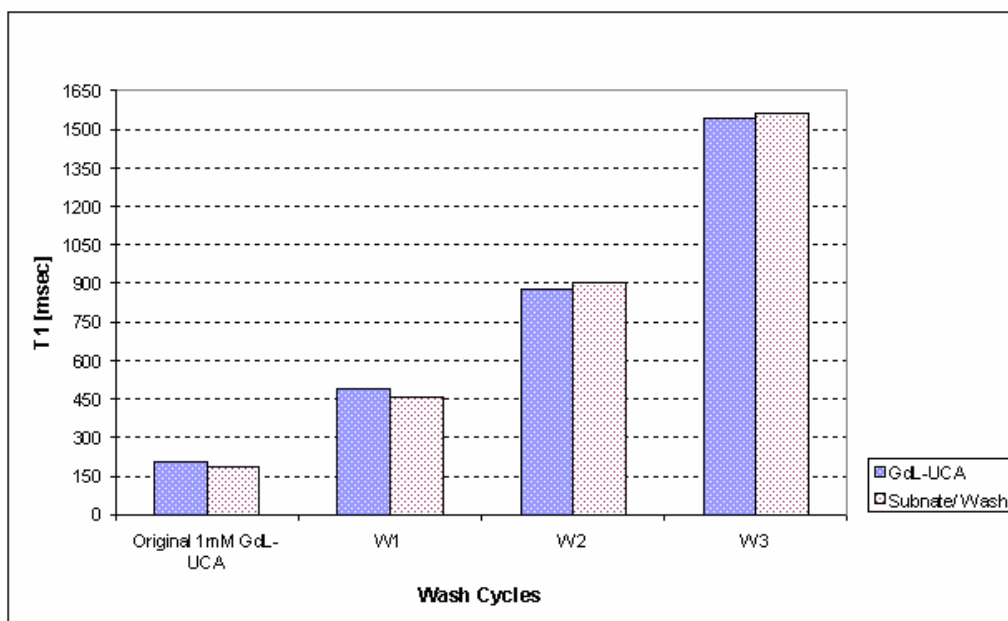
**Figure 8. Post Wash T$_1$ measurements of 1 mM GdDOTP Liposome Microbubble Suspension**

The nature of the actual GdL retention in the liposome microbubbles has yet to be determined for this set of experiments. However, it is known that the phospholipids in the liposome shell impart an overall negative charge to the microbubbles. When dissolved in water, the overall charge on a Gd-DOTA-4i-BA molecule is (+3) while the charge on a Gd-F-DOTP-ME molecule is (-1). If charge-charge interactions are behind GdL retention, then this may explain why there is a much stronger retention for the positively charged Gd-DOTA-4i-BA molecules upon subsequent washings over the Gd-F-DOTP-ME molecules. Further determination of the exact amounts of GdL incorporated into the microbubbles would involve more precise analytical chemistry approaches, such as the use of Inductively Coupled Plasma Mass Spectroscopy (ICP-MS). Based in large part on these results, a decision was made to move ahead with the next series of experiments- the use of UTMD for delivery of GdL loaded microbubbles into tissues

*3.7* *UTMD of Gd-DOTA-4i-BA into Human Fibroblast Cells and MRI*

The initial design of this experiment called for the usage of both liposome based microbubble and albumin based microbubbles for UCA loaded carriers of various Gd-based MRI contrast agents. Additionally, the whole gamut of the desired experimental outline called for timed incubations post cell GdL-UCA insonation to investigate and distinguish the UTMD/ sonoporation enhancement of GdL delivery into cells from simple cell transport based uptake of said compounds across cell membranes. Unfortunately, time constraints limited the scope of the UTMD experiments to focus on the use of albumin based microbubbles loaded with Gd-DOTA-4i-BA.

Prior to harvesting cells for UTMD experiments with the intent of acquiring MRI images, a cell viability experiment was performed to investigate possible toxic effects Gd-DOTA-4i-BA in conjunction with ultrasound would have on 3T3 cells.

The imaging protocols and UTMD methodology utilized in the final experimental procedure presented in this section, was the net result of a constantly evolving process based on several rounds of trial-and-error that often resulted in inconclusive outcomes. However, the insight gained into what went wrong (or what went right) at each step became the basis for the modifications in the subsequent approaches. A summary of these early experimental schemes and outcomes is presented towards the end of this section. The final experimental portion presented at the beginning of this section specifically focuses on the use of Optison™ mixed with solutions of Gd-DOTA-4i-BA, UTMD delivery of GdL-UCA into 3T3 cells for

comparison to a non-US cell uptake model, followed by MR imaging and $T_1$ calculations. ICP analysis was performed post imaging to determine intracellular Gd concentrations.

### 3.7.1   *Preparation of Gd-DOTA-4i-BA solutions*

A working solution of 5 mM GdL was made from powdered stock and 250 µL aliquots were withdrawn, placed into 1.5 mL eppendorf tubes and, for those samples destined to receive US, were mixed with 250 µL of Optison microbubbles. For the non-US controls, the same aliquot of GdL was mixed with 250 µL of PBS instead.  After these mixtures were added to reaction tubes containing 2 mL of cell suspension, the final GdL concentration was 0.5 mM in each reaction vessel.

### 3.7.2   *Cell Culturing*

Cells used for this experiment were NIH/3T3 mouse fibroblast cells (ATCC, Manassas, VA). In advance of the experiments, the 3T3 cells were grown in a 37° C incubator to a density of 60% confluency in a media containing DMEM (Dubleco's Modified Eagle Media, GIBCO Invitrogen, Carlsbad, CA) enriched with 10% calf serum (GIBCO Invitrogen). Harvesting of cells for experiments consisted of digestion with trypsin (GIBCO Invitrogen), suspension in the culturing media, and dilution to a concentration of $2x10^5$ cells/ mL as measured by a Coulter Counter Z3® (Beckman Coulter, Inc., Fullerton, CA)

### 3.7.3    Ultrasonication of the Cells

Cell-UCA- GdL suspensions were insonified as follows. Just before administration of the ultrasound (US), the cell suspensions were placed in sterile, round bottomed, polystyrene test tubes (17 mm, VWR Scientific, Plainfield, NJ), after which the 500 μL of GdL-Optison mixture was added to the reaction tube, followed by immersion of the reaction tubes 5 cm below the water line into a 37°C water bath, which allowed for water to surround the sample without contaminating the inside of the reaction tube. Each test tube was held at a 5 cm distance from a submerged US transducer (S3 transducer, Sonos 5500, Agilent Technology, Andover, MA) set to give a continuous 1.3-MHz US beam with a mechanical index of 1.6. All ultrasound samples received 120 sec of US exposure in the water bath. During the 120-sec insonation, the sample tube was swirled and rotated manually in the water bath every 10 sec for 3 sec duration. At the same time the US samples were being insonified, the non-US control samples were simultaneously bathed in the water bath for the same duration, but minus the 120 sec ultrasound exposure.  Immediately after the 120 s insonation, the cell suspensions that required 30 minute or more incubation were plated by pippetting the suspensions onto 35 mm polystyrene tissue culture plates (Falcon, from Becton–Dickinson Labware, Franklin Lakes, NJ) and incubated for 30, 60 and 120 minutes at 37° C. Cell suspensions to be harvested after 10 minutes remained in the reaction tubes for that time. Upon completion of the required incubation time cells were harvested by digestion with trypsin, spun down by centrifugation at 1000 rpm for 5 minutes, and followed by two successive washes with 1 mL PBS each time. After the final wash, the cells were

resuspended with 60 μL PBS for transfer into the wells of a 384 well culture plate (Falcon, from Becton–Dickinson Labware, Franklin Lakes, NJ). Wells in the 384 well-plate were loaded in the following fashion (Figure 9). The cells were then spun down by centrifugation of the 384 well-plate at 3000 rpm for 5 minutes in order to form a layer of cells at the bottom of each well for imaging purposes. The control cells received neither GdL nor Optison.
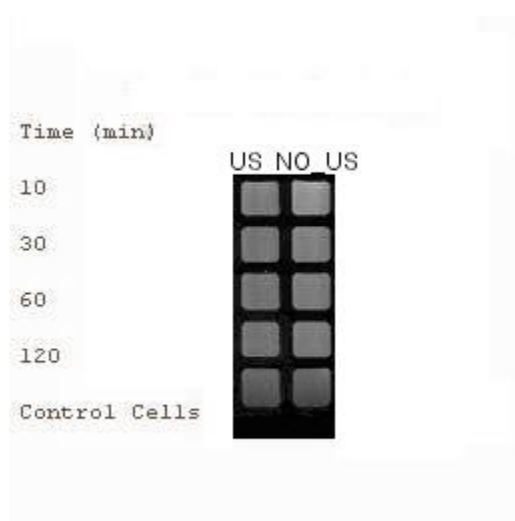


**Figure 9. 4.7T MRI Coronal Image of Cells in 384 well-plate [Time is post insonification incubation time prior to harvest]**

-US: Insonified Cells exposed to Gd-DOTA-4iBA + Optison

-NO_US: Non-Insonified Cells exposed only to Gd-DOTA-4iBA -

### 3.7.4   Cell Viability Determination

The cell viability analysis was performed at a point in the research when the focus was on incorporating GdL compounds into the synthesis of albumin microbubbles. The viability

analysis was arranged to compare insonated cells exposed to either GdL loaded into albumin microbubbles during synthesis or GdL mixed into albumin microbubbles post synthesis to non-insonified control cells. GdL loaded albumin microbubbles were synthesized using the same protocol mentioned previously with 400 μmoles of Gd-DOTA-4iBA used for synthesis. The non-loaded bubbles were synthesized by the same manner, minus the GdL. UTMD occurred by the same protocol previously described with a point of distinction being the addition of the GdL loaded microbubbles for UTMD into the 3T3 cells and each group being processed in duplicate. For these cells, 250 μL of the GdL loaded microbubbles were used. The cell concentration was 250 cells/mL yielding 500,000 cells per insonified tube. Post insonation, these cells were plated, incubated at 37° C, and observed at 1hr then 2 hr, to eventually be harvested after 24 hour incubation. Cells were then collected, pelleted at 1000 rpm for 5 minuets and resuspended in 1:1 mixture of PBS and 0.4% trypan blue stain (GIBCO Invitrogen). Non viable cells take in the blue stain making dead cells easily distinguished from living cells. Samples were taken from each replicate, counted on a hemocytometer with the percentage of viable cells defined as [(total cells - blue-stained cells)/total cells] X 100. The viability of 3T3 cells exposed to Gd-DOTA-4iBA loaded microbubbles was 91%, the viability of the microbubbles mixed with Gd-DOTA-4iBA post synthesis was 89%, while the control cells were 93% viable. The viability of those cells post UTMD differs negligibly from the control cells, 5% and 3% respectively

### *3.7.5   MR Image Acquisition and T1 Determination: Trial 1*

Cell imaging was performed in a 4.7 Tesla Varian horizontal bore magnet system using a spin-echo pulse sequence with TR (Repetition Time) values of: 0.14,  0.16,  0.2,  0.3, 0.5,  1,  2,  and 5 seconds for coronal and sagittal slice sequences. Acquired images in the form of fdf data files were then imported into ImageJ [3] for further image processing. Sagittal slices of the cell columns (Figure 10) were then used to obtain $T_1$ values using the MRI Analysis Calculator (MRIAC) plugin for ImageJ [4] and the aforementioned TR values. The MRIAC plugin uses the following algorithm (Equation 5) to generate $T_1$ values from MRI spin-echo images of signal intensity.
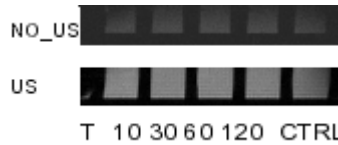


**Figure 10.  4.7T MRI Sagittal T1-Weighted Image of Insonified Cells (US) and Non-insonified Cells (NO US).  Post UTMD incubation times (min) are listed below**

$$I_n = B_0 \cdot e^{\left(\frac{-TR_n}{T1}\right)} \quad (5)$$

A pixel by pixel mapping is performed using the field strength ($B_o$), the TR value for slice n, and the measured image intensity for each pixel in slice n ($I_n$) to generate a corresponding $T_1$ calculated image.  Within this $T_1$ calculated image, regions of interest

(ROI) were selected corresponding to the 1mm thick cell layer at the bottom of each well and the $T_1$ values were determined for the cell layer.

### 3.8  Summary of Earlier UTMD Experiments & Imaging Attempts

Earlier investigations focused on trying to deliver GdL in increasing concentrations complexed with microbubbles via UTMD.  The original goal was to deliver GdL into the fibroblast cells by loading the Gd compounds into the albumin or liposome based microbubbles during microbubble synthesis. Because the early stages of this investigation were preliminary, there was not a readily accessible analytical technique available to quantify the amount of GdL that would be incorporated into the loaded microbubbles used for UTMD. The lack of this discernability was evident when trying to compare cells receiving the GdL loaded bubbles to those receiving the bubbles with GdL added separately.

### 3.8.1  Early UTMD Protocols & Initial 4.7T MRI Based Cell Imaging

The first UTMD protocol focused on delivering GdL into 3T3 cells through GdL loaded into the albumin microbubbles during synthesis. The 3 experimental cell groups consisted of the following in triplicate:

- Group A: Cells exposed to US +  1 μM Gd-DOTA-4iBA loaded into Albumin microbubbles during synthesis
- Group B: Cells exposed to US + 1 μM Gd-DOTA-4iBA added to albumin microbubbles post synthesis
- Group C: Control Cells – non-insonified, no GdL

The albumin microbubbles loaded with **Gd-DOTA-4iBA** during microbubble synthesis followed the protocol previously mentioned in section 2.2 and the UTMD protocol followed the one outlined in section 3.3 except for the use of a 70 minute post insonation incubation period before cell collection for imaging and the lack of PBS wash during collection of the cells. Cell concentrations used were 250,000 cells/mL or 500,000 cells per experimental sample. Since this was one the first attempts at MRI imaging of these cells, some ingenuity was called for in finding an optimum system for acquiring these images. Pipette tips rated for 200 μL pipettes were heat sealed shut at the delivery end by use of a soldering iron. Prior to loading these tips with the cells, the cells had to be resuspended in 1 mL of isotonic saline in the microfuge tubes they were stored in post harvesting, from which 100 μL of that suspension was transferred to the cauterized pipette tips. These tips were placed into a plastic pipette tip holder box that had been cut down in size to fit into the 6 cm diameter Quad coil used for imaging in the 4.7 T MRI scanner. Imaging results are shown in (Figure 11) and (Figure 12).
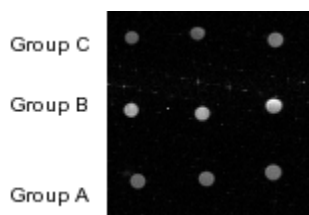


**Figure 11. 4.7T MRI Coronal Image - post UTMD of 3T3 cells**

**Group A: Cells exposed to US + 1 μM Gd-DOTA-4iBA loaded into albumin microbubbles during synthesis**

**Group B: Cells exposed to US + 1μM Gd-DOTA-4iBA added to albumin microbubbles post synthesis**

**Group C: Control Cells - non-insonified, no GdL**
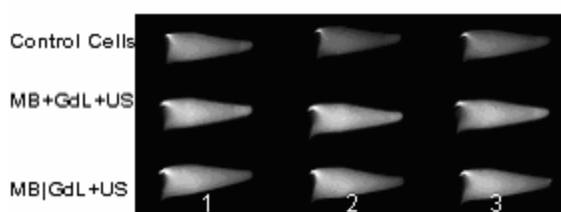
**Figure 12.  4.7 T MRI Sagittal Image of 3T3 Cells Post UTMD of Gd-DOTA-4iBA**

Because of the diluted cell suspension, the small amount of GdL used for UTMD, and the lack of a means to compact these cells into a discernable layer, the intensity of the acquired images was insufficient to draw any insight from the effectiveness of this first UTMD protocol.  The outcome of this experiment lead to protocol modification focused on delivering GdL loaded into microbubble by increasing GdL levels during the microbubble synthesis. These results should help determine an optimal GdL concentration to use for microbubble synthesis.

### 3.8.2    UTMD Protocol Modification & 400 MHz MRI Based Cell Imaging

The UTMD protocol used for this trial was based on the one outlined in chapter 3 with the emphasis here being the comparison of  GdL delivery efficiency for albumin microbubbles synthesized with 0.5 mM, 1 mM, 2 mM, and 4 mM Gd-DOTA-4iBA. GdL loaded microbubble synthesis was performed according to the protocol outlined in chapter 3. Cell concentrations utilized were 500,000 cells/mL and incubation times post UTMD were for 120 minutes.  Due to scheduling conflicts for utilizing both the clinical ultrasound machine at the North Texas VA Hospital and the MRI analyzers at the Rogers Magnetic

Resonance Center the same day, the UTMD experiments where done a week in advance, the cells harvested and frozen at -40° C, for MRI imaging the following week. Initial imaging options of harvested cells post UTMD were briefly limited to the use of the 400 MHz MRI vertical bore analyzer with an imaging coil diameter of 20 mm, due to temporary equipment malfunction on the 4.7T MRI analyzer. The use of either MRI analyzer posed a challenge as there was no preexisting protocol to follow for the imaging of small volume cell cultures, nor where there at that time any ideal tubes or containers for imaging the cells. Additionally, because of the desire to image just the cells rather then the total suspension, a method to pack to the cells down in the imaging tubes was needed. Initial efforts at finding a suitable imaging vessel involved the use of 70 mm glass melting point capillary tubes with ID of 1.5-1.8 mm. From the resuspended cells collected post UTMD, 90 µL were injected into the capillary tubes, with the tubes subsequently being spun down in a hematocrit centrifuge at 1000 rpm for 10 min. The injection processes it self proved to be time consuming, difficult, and ultimately inconsistent. Strips of 10 gage polyethylene tubing were attached to gel loading micropipette tips, and inserted down into the capillary tubes in order to fill the tubes from the bottom up so as to avoid air bubble formation. Even with slow, steady injection from the micropipette, air bubbles were frequently introduced into the capillary tubes either necessitating the spinning down of the not fully loaded tubes before further addition, or tube overflow leading to cell loss. As a result of these difficulties, not all of the tubes were loaded with equal volumes of cells. Additionally, the lack of a sufficient cell concentration used for each sample necessitated the pooling of the triplicates into one tube for imaging.

After packing down the cells by centrifugation, the tubes were evenly aligned and tapped to a glass microscope slide, then placed into the sample holder for insertion into the 400 MHz MRI spectrometer. Using a spin-echo pulse sequence for coronal and sagittal sequences, cell imaging was performed. The coronal image is shown in (Figure 13).



Ctrl 0.5 1 2 4

**Figure 13. 400MHz MRI Coronal Image of 3T3 Cells Post UTMD Delivery of Gd-DOTA-4iBA Sequence: Control Cells, 0.5mM, 1mM, 2mM, 4mM Gd-DOTA-4iBA [used in microbubble synthesis]**

$T_1$ calculations were obtained using ImageJ and the MRIAC plugin and are displayed in Table 2. The observed $T_1$ values are inline with expectations, as the cells undergoing UTMD with microbubbles synthesized with higher levels of GdL exhibit shorter $T_1$ values than those undergoing UTMD with lower GdL concentration microbubbles.

**Table 1: $T_1$ Values for 3T3 Cells Post UTMD at 400MHz MRI**

| Sample [GdL]mM | $T_1$ [sec] |
|---|---|
| 0 – ctrl | **2.193** |
| 0.5 | **1.685** |
| 1 | **1.362** |
| 2 | **0.986** |
| 4 | **0.584** |

# CHAPTER FOUR
## Results & Discussion

### 4. <u>Imaging Results Trial 1</u>

$T_1$ values acquired from ImageJ-- MRIAC are displayed (Figure 14). Excluding the cells harvested after 10 minutes post insonification, there appears to be a trend showing an association between incubation time in the presence of GdL and a shortening of the $T_1$ value. The largest differences appear to be between cell samples harvested after 30 minutes and after 60 minutes incubation time, with a percent difference of 16.15% from the 30 minute incubated insonified to the non-insonified cells and a 21.13% difference between the same cells harvested after 60 minute incubation. Without being able to model the method of GdL internalization into the cells, Equation 2 becomes inoperable in calculating intracellular GdL concentrations.
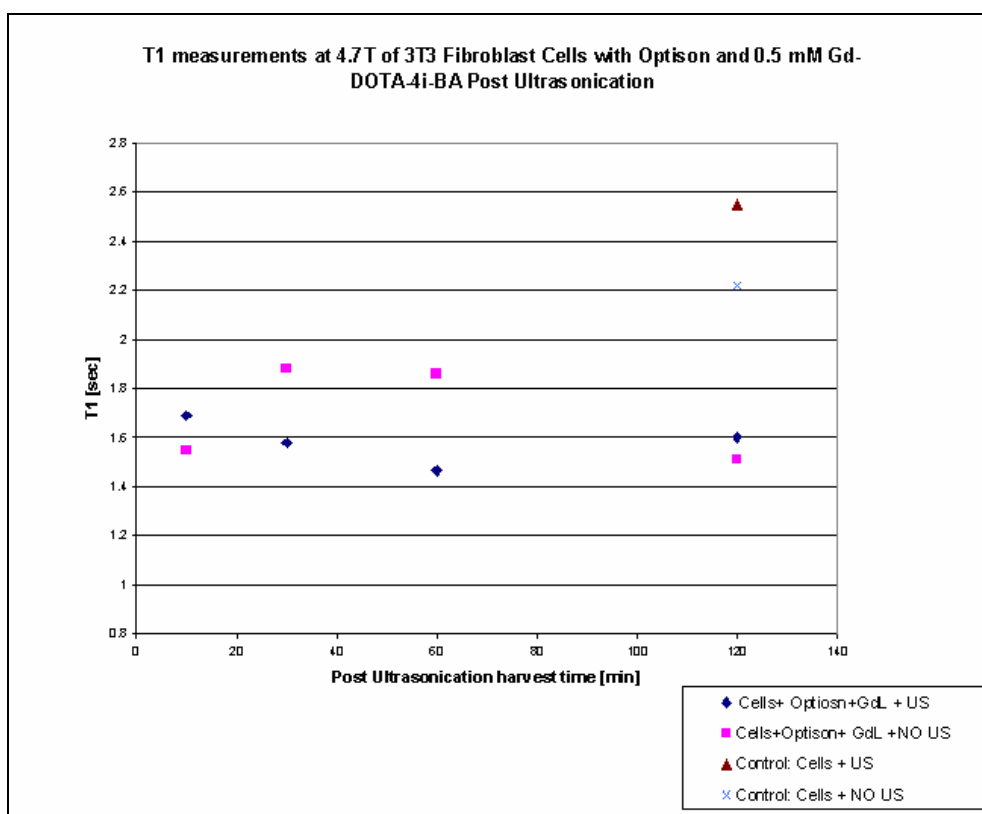
**Figure 14. $T_1$ measurements at 4.7T of 3T3 Fibroblast Cells with Optison and 0.5 mM Gd-DOTA-4i-BA Post Ultrasonication**

## 4.1 Discussion: Trial 1

These experimental procedures do not provide clear enough results to draw any statistically solid conclusions regarding the nature of ultrasound enhanced uptake of the GdL into the fibroblast cells. With that said, there is an observed time dependent uptake displayed with the $T_1$ shortening as the incubation time increased over the first hour. Though the cells were exposed to the GdL in the media during the incubation times, which would allow for

some cell membrane association, post cell harvest washings with PBS would remove most of the loosely associated GdL particles. Therefore, some form of active cellular uptake of the GdL compounds must be occurring to explain the shortening $T_1$ observation. This occurrence of lanthanide conjugate transport into cells has been explored in detail by other researchers [5]. More experiments need to be performed to validate this including a time point analysis of cells incubated with an array of GdL compounds to see if UTMD enhances GdL uptake efficiency in the cells to a significantly distinguishable level from normal endocytosis or active transport mechanism uptake, although the current literature suggests the likelihood of the later mechanism. Active cell uptake may explain why both the insonified and non-insonified cells harvested after 120 minutes have minimal noticeable difference between their respective $T_1$ values. Noise corrupts the image acquisition process more noticeably when trying to obtain MRI image slices with thicknesses less then 2 mm, so having a cell layer at the bottom of the wells in excess of 2 mm facilitates quality MRI image acquisition. Further insight into the mechanisms most responsible for UTMD delivery of GdL agents into tissues would come about by comparing GdL delivery efficiency of insonified cells with microbubbles present and without. Such experiments may isolate the role of sonoporation effects alone in GdL uptake into tissue cells. UTMD gene therapy research has demonstrated an observable increase in transfection efficiency for naked DNA in tissues exposed to ultrasound without a UCA carrier over non-insonified controls [2].

## 4.2    UTMD of Gd-DOTA-4i-BA into Fibroblast Cells & MRI Imaging: Trial 2

With the observations and lessons learned from trial one, a second UTMD experiment was performed. However, the focus of this second trial was on the zero time point comparison, with the cells being harvested immediately post insonation. The choice of this immediate analysis was called for by a need to minimize cell exposure time to GdL therefore minimizing, in theory, cell transport based internalization of the Gd compound. Additionally, these experiments were run in triplicate, with a 3$^{rd}$ experimental group added in the form of 3T3 cells insonified in the presence of 0.5 mM Gd-DOTA-4iBA minus the Optison microbubbles. All the previous protocols from trial 1 were used with the only modifications being the lack of post UTMD incubation time and increasing the utilized cell concentrations to $3x10^6$ cells/mL. Upon completion of the UTMD portion of this trial, the cells were collected and placed into a 396 microwell plate, as before, for imaging & $T_1$ determination. The three experimental cell groups were categorized as such:

- Group A: Cells exposed to US + Gd-DOTA-4iBA+ Optison
- Group B: Cells exposed to Gd-DOTA-4iBA only
- Group C: Cells exposed to US + Gd-DOTA-4iBA minus Optison

### 4.2.1    MRI Imaging Results: Trial 2

The cell imaging was performed in the same manner as previously detailed.  Sagittal images (Figure 15) were used again for $T_1$ determination using ImageJ and the MRIAC plugin. A distinct, bright cell layer is observed in the bottom of the wells. The extracted $T_1$

values are displayed in (Figure 16). Observed values for groups A & B are similar to the values observed after 10 minute post UTMD incubation in trial 1 with group A exhibiting average $T_1$ value of 1.39±0.03 sec (similar to 1.69 sec from trial 1 for insonified cells) and group B having average $T_1$ value of 1.46±0.01 sec (comparable to 1.55 sec from trial 1 for non-insonified cells).
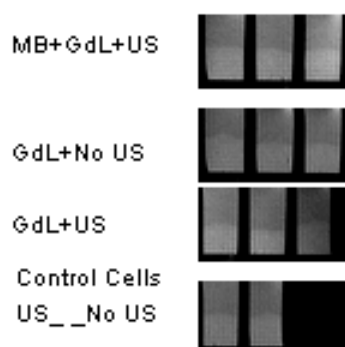


**Figure 15.   4.7T MRI $T_1$ Weighted Sagittal Images of 3T3 Cells Post UTMD**
**Insonified Cells (US) in the Presence of 0.5mM Gd-DOTA-4iBA (GdL) and Optison Microbubbles (MB)**
**Non-insonified Cells (NO US) in the Presence GdL**
**Insonified Cells (US) in the Presence of GdL minus MB**
**Insonified & Non-Insonified control cells**
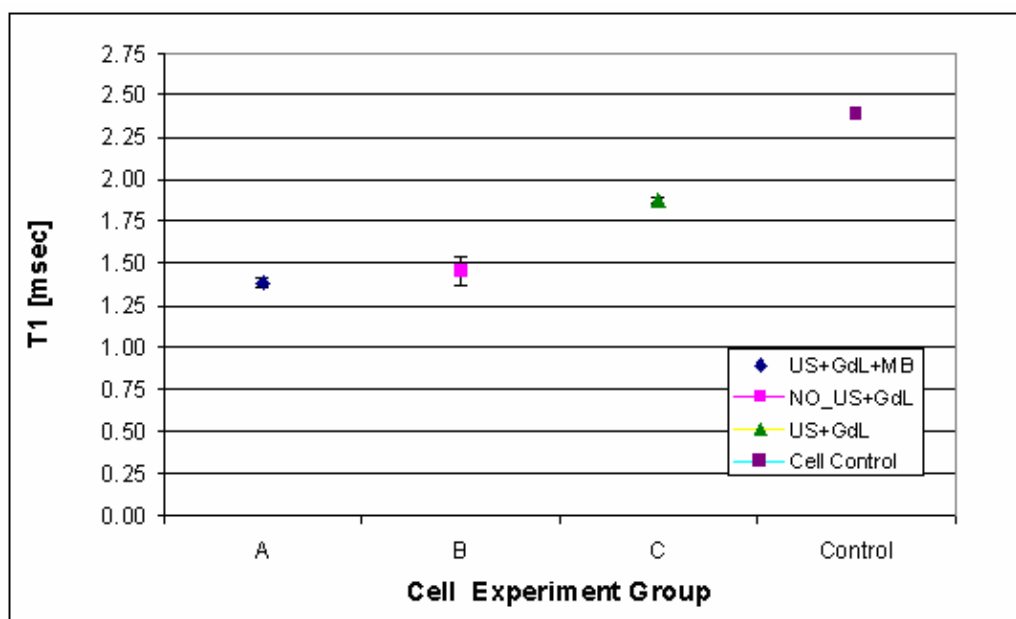
**Figure 16. Post UTMD $T_1$ measurements at 4.7T of 3T3 Fibroblast Cells with 0.5 mM Gd-DOTA-4i-BA**

### 4.2.2  Inductively Coupled Plasma - Mass Spectrometry (ICP-MS) Analysis

Upon completion of acquiring MRI images of the cells, the cells were prepared for **inductively coupled plasma - mass spectrometry (ICP-MS)** analysis in order to determine the precise concentrations of GdL delivered by UTMD (or cell transport) into the cells.

### *4.2.2.1   Background: Inductively Coupled Plasma - Mass Spectrometry (ICP-MS)*

ICP-MS is an exquisitely sensitive ultra-trace element detection technique providing for rapid multi-element determinations. For many trace elements, the sensitivity of ICP-MS can be as low as 0.1-1 parts per trillion (ppt) range.  Although a number of different ICP-MS configurations exist, all share the same common components: the nebulizer, spray chamber, plasma torch, interface, and detector. Where each configuration differs is in the design of the mass spectrometer, particularly the arrangement of the mass separation device. In brief, the concept behind ICP-MS analysis is that elements in solution are aspirated in to a nebulizer which atomizes the solution in an aerosol carried by argon gas. Next, the atomized solution enters a spray chamber where the smaller droplets of the aerosol are separated out and directed into an intense magnetic field (produced by [RF] passing through a copper coil) before entry into a concentric quartz tube torch. In the plasma torch, the now ionized gas exits as very high temperature plasma discharge (~10,000 K). Positive ion species generated in by the plasma torch are swept into the vacuum environment of the mass spectrometer through an interface region.  Once inside the mass spectrometer, ions are separated by their mass to charge ratios using a quadrupole spectrometer.

### 4.2.3  ICP-MS Sample Preparation

Post MRI analysis the 100 μL of 3T3 cells in PBS where extracted from the microwells and lysed in 900 μL of a 0.5% triton solution. Since the element being detected is the Gd inside the cells, the detergent induced cell lysis should help to liberate the internalized Gd into solution.  Requirements for ICP-MS sample preparation necessitated diluting the sample in excess ultra-pure 4% HNO3 in order to dissolve away most of the organic matter, keep the cationic species in a solubilized form, while diluting the total Gd concentration into the range of the calibrated reference standards: 0.1, 1, 10, & 100 parts per billion (ppb). The theoretical maximal Gd content of the unlysed cells (assuming a highly improbable 100% transfer of GdL into the cells post UTMD) was calculated to be in the range of 300-400 ppm. With the dilution factor of the triton solution taken into consideration, 50 μL of the lysed cell- triton solution was further diluted into 15 mL of 4% HNO3 to bring the final theoretical Gd concentration far below the target reference value of 10 ppb. The 10 ppb reference standard was necessitated since the protocol for ICP-MS analysis requires that after every 3rd sample being investigated, a reference standard must be analyzed, so that instrumental drift can be corrected for. Additionally, this reference value is considerably greater then the theoretical transferred amount of Gd into the highly diluted cell suspension, but still within 1-2 orders of magnitude of the likely transferred amount.

### 4.2.4  ICP-MS Analysis Results

The prepared specimens were analyzed on a Perkin Elmer Sciex Elan 6100 DRC (PerkinElmer Life and Analytical Sciences, Shelton, CT USA), which was kindly provided

by the research lab of  Dr. Mathew Leybourne at the University of Texas at Dallas. The normal automated sampler was not working during the time this analysis was performed, so the samples had to be introduced into the sampler by hand. The detected concentrations of Gd in the samples are recorded in parts per trillion (ppt) on the PC interfaced to the ICP-MS. An instrumental drift of 1.9% was observed over the course of the analysis and thus a correction was performed on the observed data. These observations were then converted back into the corresponding micro molar values of the original cell samples.  .  Averaged values for each experimental group are displayed in (Figure 17)
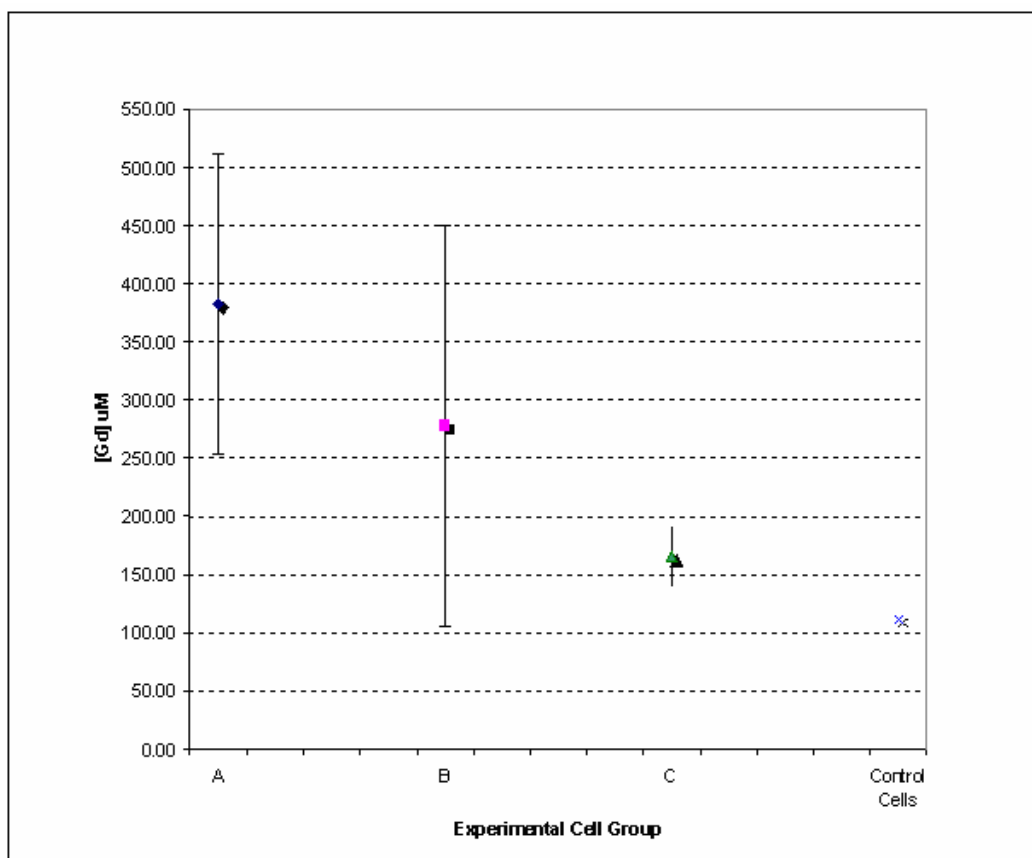


**Figure 17. ICP-MS Determination of [Gd] Delivered Into 3T3 Cells via UTMD**

The average of the three replicates for group A contain 382.68 ± 129.08 μM Gd. Non-insonified cells, group B, were observed to contain 277.47 ±171.85 μM Gd while the cells in group C incorporated 165.45 ± 25.73 μM Gd. Statistical analysis using the t-test with assumed equal variance revealed there was no statistical difference between the means of group A and group B using the protocol outlined in this experiment. The same was true for a comparison between group A and group C. Only one cell control was analyzed.

### 4.2.5 ICP-MS Analysis Discussion

The range of values observed for the cells in groups A & B imply there is only slight if any observed enhancement gained by the use of UTMD in loading 3T3 cells with Gd-DOTA-4iBA. However, there is a distinct difference between the cells of group C, the insonified cells minus microbubbles, and the other two groups. The large range of values observed in the first two groups, standard deviations of 34% and 62% respectively, is one the drawbacks to using so few members, n=3, for each group in cell experiments such as these. To elaborate on this, it would appear that the cell lysis step using 0.5% triton was unnecessary, as was the final dilution amount. The volume of cells utilized for this experiment would have been adequately broken up by the 4% HNO3 solution itself, even at a final dilution of half the one used and still be below the reference range of the standard. The amount of cells possibly lost by the combined effects of insonation, PBS washing, followed by the ICP-MS sample preparation and over dilution, may have induced some variability among the cell amount in the members of each group. The noticeable level Gd detected in the

control sample is probably an aberration that occurred by using the control cells plated in the imaged microwell plate, as the observed  T1 values of the cell controls indicate no significant amount of Gd should be present. These cells may have received some inadvertent splash over from the neighboring well during the process of injecting the 3 members of the non-insonified group B. This would have best been avoided by using control cells that had not been placed into the imaging microwell plate

.

# CHAPTER FIVE

## Conclusions

The inconclusiveness of the imaging approaches outlined here to determine UTMD enhancement of 3T3 intracellular incorporation of GdL compounds implies that MRI analysis may not be the best detection modality. A better approach may be **fluorescence microscopy** examination of intracellular uptake of the Eu and Tb complexed versions of the macrocyclic ligands under investigation. This method of microscopy allows for time course examinations that require fewer cells per experiment then the MRI detection protocol outlined in this paper. Fluorescence microscopy also allows for precise determination of which compartments in the cell the internalized Ln compounds have gone. When performed in conjunction with ICP-MS, a complete picture of the amount of Ln complex delivered into the cells and the internal compartmentalization of said compound may be realized.

In summary:

1. Incorporation of 5mM solutions of Gd based MRI contrast agents, Gd-F-DOTP-ME and Gd-DOTA-4i-BA, into liposome microbubbles was successively performed. The GdL compounds exhibited strong association to the liposome microbubbles as GdL retention was still observed after multiple PBS washes and $T_1$ measurements at 20 MHZ. The use of these GdL loaded liposome microbubbles for UTMD delivery into tissue is still work in progress.

2. Delivery of Gd-DOTA-4i-BA by UTMD with Optison™ into 3T3 fibroblast cells shows negligible improvement over non-insonified controls. Observed $T_1$ values at

43

4.7 T are observed to be shorter for the cells undergoing UTMD versus the controls. Additionally, an exposure time relationship is shown with both insonified and non-insonified 3T3 cells incubated with Gd-DOTA-4i-BA displaying a shortening of $T_1$ values the longer the cells are incubated with the GdL.

3. **Inductively Coupled Plasma - Mass Spectrometry (ICP-MS)** analysis of 3T3 cells post UTMD delivery of 0.5 mM Gd-DOTA-4i-BA reveals the concentrations of Gd delivered into the cells to be $382.68 \pm 129.08$ µM, but does not detect any statistically significant difference in Gd concentration from the non-insonified controls.

# BIBLIOGRAPHY

1.      Frenkel, P.A.C., Shuyuan Thai, To Shohet, Ralph V. Grayburn, Paul A., DNA-loaded albumin microbubbles enhance ultrasound-mediated transfection in vitro., in Ultrasound in Medicine & Biology. 2002. p. 817.

2.      Shohet, R.V., et al., Echocardiographic Destruction of Albumin Microbubbles Directs Gene Delivery to the Myocardium. Circulation, 2000. 101(22): p. 2554-2556.

3.      Burns, P.N. and H. Becher, Handbook of Contrast Echocardiography: LV Function and Myocardial Perfusion. 2000, Frankfurt & New York: Springer Verlag. 200.

4.      Raisinghani, A. and A.N. DeMaria, Physical principles of microbubble ultrasound contrast agents. The American Journal of Cardiology, 2002. 90(1): p. 3-7.

5.      Barnett, S.B., et al., The sensitivity of biological tissue to ultrasound. Ultrasound in Medicine & Biology, 1997. 23(6): p. 805-812.

6.      AIUM, Section 3--selected biological properties of tissues: potential determinants of susceptibility to ultrasound-induced bioeffects. American Institute of Ultrasound in Medicine. J Ultrasound Med, 2000. 19(2): p. 85-96.

7.      Abramowicz, J.S.M., Morton W. Battaglia, Linda F. Mazza, Salvatore, Comparative hemolytic effectiveness of 1 MHz ultrasound on human and rabbit blood in vitro., in Ultrasound in Medicine & Biology. 2003. p. 867.

8.      AIUM, Section 2--definitions and description of nonthermal mechanisms. American Institute of Ultrasound in Medicine. J Ultrasound Med, 2000. 19(2): p. 77-84.

9.      Riesz, P. and T. Kondo, Free radical formation induced by ultrasound and its biological implications. Free Radical Biology and Medicine, 1992. 13(3): p. 247-270.

10.     AIUM, Section 6--mechanical bioeffects in the presence of gas-carrier ultrasound contrast agents. American Institute of Ultrasound in Medicine. J Ultrasound Med, 2000. 19(2): p. 120-142.

11.     Miller, M.W., D.L. Miller, and A.A. Brayman, A review of in vitro bioeffects of inertial ultrasonic cavitation from a mechanistic perspective. Ultrasound Med Biol, 1996. 22(9): p. 1131-54.

12.     AIUM, Section 5--nonthermal bioeffects in the absence of well-defined gas bodies. J Ultrasound Med, 2000. 19(2): p. 109-119.

13.     Guzman, H.R., et al., Bioeffects caused by changes in acoustic cavitation bubble density and cell concentration: a unified explanation based on cell-to-bubble ratio and blast radius. Ultrasound in Medicine & Biology, 2003. 29(8): p. 1211-1222.

14.     Girod, G., et al., Cavitation versus Degassing: In Vitro Study of the Microbubble Phenomenon Observed During Echocardiography in Patients with Mechanical Prosthetic Cardiac Valves. Echocardiography, 2002. 19(7): p. 531-536.

15.     Caravan, P., et al., Gadolinium(III) Chelates as MRI Contrast Agents: Structure, Dynamics, and Applications. Chem Rev, 1999. 99(9): p. 2293-352.

16.     Sherry, A.D., et al., The Gd(3+) complex of a fatty acid analogue of DOTP binds to multiple albumin sites with variable water relaxivities. Inorg Chem, 2001. 40(26): p. 6580-7.

17.     Rasband, W., ImageJ, NIH: Bethesda, Maryland.

18.     Schmidt, K., MRI Analysis Calculator Plugin (for ImageJ). 2002, HypX Laboratory.

19.     Frias, J.C., et al., Luminescent nonacoordinate cationic lanthanide complexes as potential cellular imaging and reactive probes. Org Biomol Chem, 2003. 1(6): p. 905-7.

# VITAE

C. Hunter Russell III was born in Dallas, Texas on March 3, 1972, the son of Cline H. Russell Jr. and Julia L. Russell. Upon graduating from Nimitz High School, Irving, Texas in 1990, he worked various jobs while attending college part-time at local campuses in the Dallas Community College District. He received his Associates of Arts and Sciences in June of 1998, at which time he entered the University of Texas at Dallas. He received a Bachelor of Arts in Biology in June of 2000. The following Fall he entered into the University of Texas at Arlington—University of Texas Southwestern Medical Center at Dallas joint program in Biomedical Engineering to pursue a Masters of Science. He was awarded a Masters of Science degree in June 2004.

Permanent Address:   2709 SPRINGLAKE Ct.
                     IRVING, TX 75060